Physica C: Superconductivity and its applications 583 (2021) 1353853

Contents lists available at ScienceDirect

Physica C: Superconductivity and its applications

journal homepage: www.elsevier.com/locate/physc

The instantaneous dynamic resistance voltage of DC-carrying REBCO tapes to AC magnetic field

Chao Li [a], Yuying Xing [a,*], Jiabin Yang [b], Fengrui Guo [c], Bin Li [a], Ying Xin [a], Boyang Shen [b,*]

[a] School of Electrical and Information Engineering, Tianjin University, Tianjin 300072, China
[b] Electrical Engineering Division, Department of Engineering, University of Cambridge, Cambridge CB3 0FA, United Kingdom
[c] Tianjin Dongli Electric Power Supply Company, State Grid, China

ARTICLE INFO

Keywords:
Dynamic resistance
AC magnetic field
REBCO tape
DC component
Fourier expansion

ABSTRACT

When a REBCO tape carrying DC transport current is exposed to a perpendicular AC magnetic field with amplitude above certain value, flux could be triggered to traversing the superconducting tape. During the process, a biased DC response voltage, called the dynamic resistance voltage will be induced. In the paper, the calculation on the time-dependent dynamic resistance voltage was carried out by the ***H***-formulation model implemented in the finite-element method (FEM) software package COMSOL Multiphysics. Fourier analysis on the waveform of dynamic resistance voltage was utilized to figure out the main components of the response voltage. The DC component, second harmonic component and ratio of the two components can reflect how the instantaneous dynamic resistance responds to the applied AC magnetic field and the DC transport current. The findings in the paper can be used to monitor the state of DC-carrying REBCO tapes subject to an AC magnetic field.

1. Introduction

With the rapid progress in manufacturing REBCO coated conductors with high current-carrying capability, extensive interest has been stimulated in the development of high temperature superconducting (HTS) devices such as transformers [1], rotating motors [2], fault current limiters [3-4] and high-field magnets [5]. In above applications, it is unavoidable that the REBCO tapes carry DC transport currents in the background of AC magnetic fields.

Under the situation, an interesting phenomenon called "dynamic resistance effect" has been discovered accordingly [6-8]. Specifically, a time-dependent DC electrical field will be induced in the superconductor carrying DC transport current even below its critical current. The DC electrical field actually origins from certain amount of net flux, induced by external field, traversing across the superconductor from one side to the either side. It is the interaction between the net flux and the DC transport current that generates the electrical field. Since the electrical field is in the same direction of the DC transport current in the superconductor, some power dissipations will be generated. A virtual resistance could be introduced to be responsible for the power dissipation and the virtual resistance is called dynamic resistance [9-11]. Correspondingly, the across the superconducting tape is called dynamic resistance voltage.

The dynamic resistance, on one hand, will lead to heat dissipation [24], and even impose a heavy burden on the cryogenic system for superconducting devices [12]. On the other hand, it can be utilized to energize superconducting coils in HTS flux pumping systems [13–16]. Some theoretical analysis and mathematical methods were developed in [17–19] to calculate the dynamic resistance. Simulation model for the dynamic resistance was built in [20-22].

Most of previous research focused on the time-averaged dynamic resistance rather than the instantaneous dynamic resistance. However, the instantaneous dynamic resistance actually reflects the state of the superconductor in real time. In this paper, a detailed investigation on the instantaneous dynamic resistance voltage of REBCO tapes to the AC magnetic field considering the multi-layer structure has been carried out. The waveform of the dynamic resistance voltage has been described under different external conditions through a FEM model based on the ***H***-formulation. Fourier expansion has been applied to analyze the instantaneous dynamic resistance voltage, providing an insight into how the dynamic resistance voltage responds to the applied AC magnetic field and the DC transport current in the superconductor.

* Corresponding authors.
E-mail addresses: 18842500260@163.com (Y. Xing), bs506@cam.ac.uk (B. Shen).

https://doi.org/10.1016/j.physc.2021.1353853
Received 25 February 2021; Accepted 7 March 2021
Available online 9 March 2021

2. Dynamic resistance voltage and its simulation model based on finite element method

2.1. The Dynamic Resistance Voltage of DC-carrying REBCO Tapes to AC magnetic Field

The dynamic resistance effect refers to the phenomenon that a slab-like superconductor, under the background of AC magnetic field, could present a resistance even if its DC transport current is less than the critical current. Oomen [11] proposed a mathematical equation which could explain how to calculate the dynamic resistance in a superconductor, as shown in (1):

$$R_{dyn} = \frac{4alf}{I_{c0}}\left(B_a - B_{a,th}\right) \tag{1}$$

Where 2a is the width of the superconducting slab, l is the length of the superconductor, f is the frequency of the applied ac magnetic field, B_a is the magnitude of the applied ac magnetic field and $B_{a,th}$ is the threshold of the magnetic field that can fully penetrate the superconductor.

Due to the dynamic resistance effect, a DC response voltage will appear with DC transport current flowing through the superconducting slab. According to (1), the dynamic resistance voltage should be constant if the geometry of the superconducting slab, the applied AC magnetic field and the DC transport current are fixed. However, it can be observed that that value of the dynamic resistance voltage varies with time periodically in the experiment. This is because the value of the dynamic resistance calculated by (1) is a root mean square (RMS) value rather than an instantaneous value.

In fact, the time-dependence phenomenon of the dynamic resistance voltage results from the flux motion periodically triggered by applied AC magnetic field in the superconductor. As shown in Fig. 1(a), if the applied AC magnetic field is below the threshold field, no net flux could traverse the superconductor and no dynamic resistance voltage occurs. Fig. 1 (b) describes the circumstance that the applied AC magnetic field is capable of fully penetrating the superconductor. During each cycle of the AC field, a certain amount of flux will transfer from one side of the superconductor to the other side, through traversing across the central region of the superconductor where DC transport current flows. This process is hysteretic. In the process, the dynamic resistance voltage is expressed by (2):

$$\begin{aligned} \frac{V_{up}}{L} &= a\frac{I_{trans}}{I_c}\frac{dB}{dt} \qquad if\ \Delta B > 2B_{a,th} \\ \frac{V_{up}}{L} &= -a\frac{I_{trans}}{I_c}\frac{dB}{dt} \qquad if\ \Delta B < -2B_{a,th} \end{aligned} \tag{2}$$

According to (2), the dynamic resistance voltage will achieve the maximum value for two times in one cycle of the applied AC magnetic field. Correspondingly, the curve of the instantaneous dynamic resistance voltage should show the characteristic of two peaks, which appear where d$\boldsymbol{B}$/dt is the largest.

2.2. The DC Component and Second Harmonic Component in the Dynamic Resistance Voltage

The waveform of the dynamic resistance voltage can be expressed in the form of Fourier expansion, as shown in (3). As previously described, an important feature of the dynamic resistance voltage waveform is that two voltage peaks appear in one cycle of the applied AC field. The feature indicates that a biased DC component and secondary harmonic component are mainly contained, assuming the frequency of the applied AC field is considered as the fundamental frequency.

$$u(t) = \mathrm{C}_0 + \sum_{n=1}^{\infty}\left(a_n\cos(2\pi nft) + b_n\sin(2\pi nft)\right) \tag{3}$$

Where

$$C_0 = \frac{1}{T}\int_0^T u(t)dt, a_n = \frac{2}{T}\int_0^T u(t)\cos(2\pi nft)dt, b_n = \frac{2}{T}\int_0^T u(t)\sin(2\pi nft)dt$$

The DC component and second harmonic component will change as the dynamic resistance voltage varies. And the dynamic resistance voltage will be impacted by the applied AC field or the DC transport current. Therefore, it's necessary to carry out investigation on how the DC component and the second harmonic component respond to external conditions and whether the response could be utilized to indicate the state of the superconducting tape under AC magnetic field.

2.3. Simulation Model on the Finite Element Method

Finite-element method is used to calculate and display the waveform of the dynamic resistance voltage. The dynamic resistance voltage of a REBCO tape is simulated using the finite element multi-layer architecture shown in Fig. 2. The HTS superconductor layer is sandwiched between two layers of stabilizer made of copper. External AC magnetic field is applied perpendicular to the REBCO tape along the y-axis. The DC transport current flows in the REBCO tape along the z-axis.

The mathematical calculations are based on a 2D $\boldsymbol{H}$-formulation model [23], where the governing equations are derived from Maxwell's equations, such as Faraday's law (4) and Ampere's law (5).

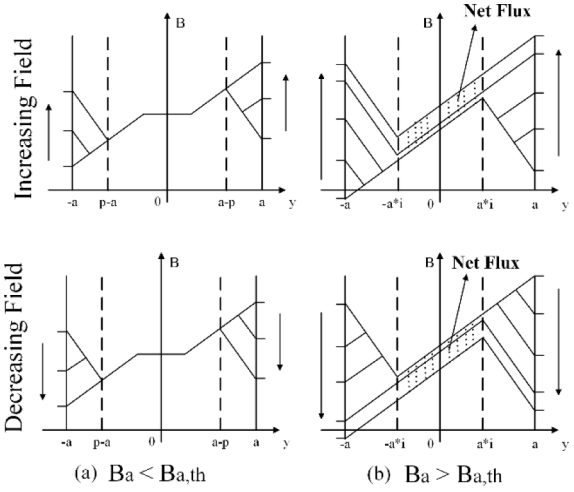

Fig. 1. Schematic drawing of the REBCO tape with multi-layer structure under AC magnetic field.

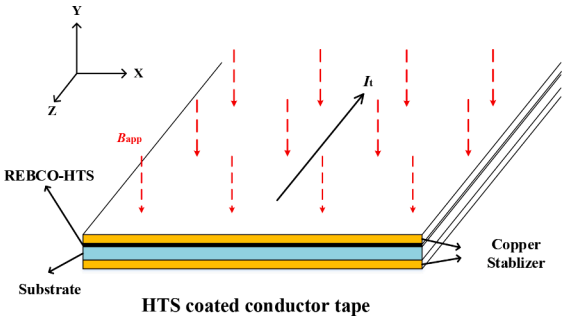

Fig. 2. Schematic drawing of the REBCO tape with multi-layer structure under AC magnetic field.

$$\nabla \times E + \frac{dB}{dt} = \nabla \times E + \frac{d(\mu_0 \mu_r H)}{dt} = 0 \tag{4}$$

$$\nabla \times H = J \tag{5}$$

where $\boldsymbol{E}$ is the electric field, $\boldsymbol{B}$ is the magnetic flux density, $\boldsymbol{H}$ is the magnetic field intensity, $\boldsymbol{J}$ is the current density, μ_0 is the permeability of free space and μ_r is the relative permeability. The Equation (6) presents the $\boldsymbol{E}$-$\boldsymbol{J}$ power law considering field dependent critical current model and gives an insight to the electrical properties of REBCO tapes.

$$E = \frac{E_0}{J_c(B,\theta)} \left| \frac{J}{J_c(B,\theta)} \right|^{n-1} J \tag{6}$$

Where J_c is the critical current density, n is the power factor of superconducting tape. It is assumed that electric field E_z is parallel to the current density J_z. Through combining (4), (5), (6), a partial differential equation with variable $\boldsymbol{H}$ could be established and solved in the COMSOL Multiphysics software package [25,26]. The parameters of the simulation model are shown in Table 1.

3. Simulation results and analysis

3.1. The Impact of the AC Magnetic Field on the Dynamic Resistance Voltage of REBCO Tape

The waveforms of the dynamic resistance voltage can be obtained from the numerical simulations using the $Jc(\boldsymbol{B})$ model which has been introduced in Section II. Fig. 3 shows the waveforms of the dynamic resistance voltage for DC transport current $I_{trans} = 0.5\, I_c$ over two cycles of a 50 Hz AC magnetic field. The amplitude B_{app} of the AC magnetic field is 20 mT, 50 mT, 75 mT and 100 mT respectively. It can be observed that the waveforms of the dynamic resistance voltage always maintain positive despite some fluctuation, which suggests that the power dissipation is generated during the process. The dynamic resistance voltage is positively related to the amplitude of the applied AC magnetic field. There are two maximum values of the dynamic resistance voltage in one cycle of the applied AC field and they approximately happen around the region where $|d\boldsymbol{B_{app}}/dt|$ is relatively large. All of above characteristics complies with (2).

From the perspective of the Fourier expansion, the DC component and second harmonic component of the dynamic resistance voltage in Fig. 3 could be obtained through (3). As shown in Fig. 4, the blue curve, the green curve and red curve represent the DC component, second component and the ratio of the two components respectively. Both of the two components increase with the amplitude of applied AC field going up. It's obvious that the DC component increases much faster than the second harmonic component, causing the ratio of the two components to increase as well. Hence, the ratio of the two components is positively related to the amplitude of the AC magnetic field.

Then, we investigated the impacts of frequency of applied AC fields on the dynamic resistance voltage of superconductors. Simulations are carried out in the scenario where the frequency of AC fields is set to be 25 Hz, 50 Hz, 100 Hz, 500 Hz and 1000 Hz respectively. The DC component and second harmonic component are shown by the blue curve with solid triangle and the green curve with hollow triangles in Fig. 5. Both of the two components scaled up with the frequency of AC fields, indicating the dynamic resistance voltage is in proportion with the frequency. However, the ratio of the two components, shown by the red curve with circles, stays almost stable despite the increasement of the two components.

Table 1
The parameters of the simulation model

Parameters	Value
Width of the superconducting tape	4mm
Thickness of Superconducting layer	1μm
Thickness of Copper layer	100μm
Tape Self-field I_c at 77 K	85.5A
F	50Hz
μ_0 n (E-J Power Law index) E_0	$4\pi \times 10^{-7}$H/m 29 10^{-4}V/m

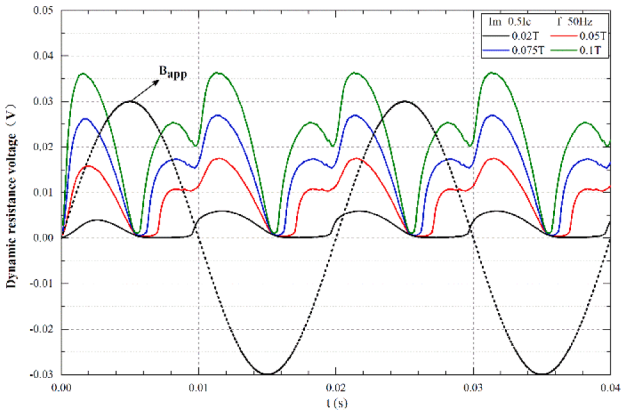

Fig. 3. The instantaneous dynamic resistance voltage of the REBCO tape for 0.5Ic transport current under the 50hz AC magnetic fields with amplitude $|B_{app}|$= 20 mT, 50 mT, 75 mT and 100 mT.

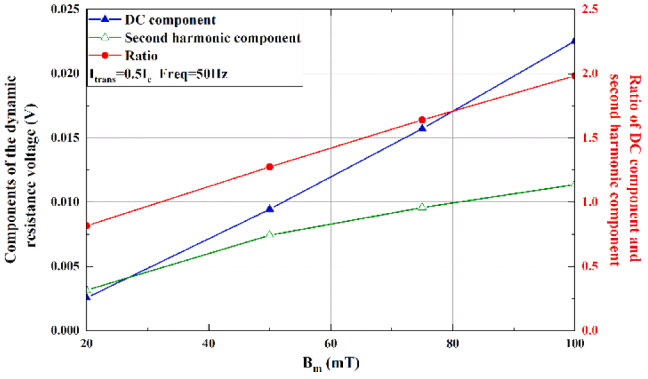

Fig. 4. The DC component, second harmonic component and ratio of the DC component and second harmonic component for the dynamic resistance voltage of REBCO tape with 0.5Ic transport current under 50 Hz AC magnetic fields with amplitude $|B_{app}|$= 20 mT, 50 mT, 75 mT and 100 mT.

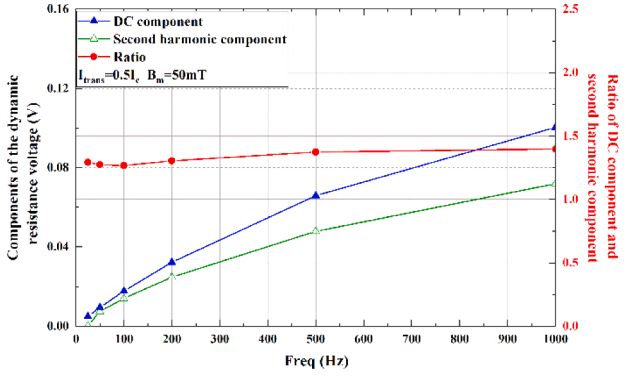

Fig. 5. The DC component, second harmonic component and ratio of the DC component and second harmonic component for the dynamic resistance voltage of REBCO tape with 0.5Ic transport current under 50mT AC fields with frequency f=25 Hz, 50 Hz, 100 Hz, 200 Hz, 500 Hz and 1000 Hz.

3.2. The Impact of DC Transport Current on the Dynamic Resistance Voltage of REBCO Tape

Fig. 6 presents the dynamic resistance voltage of the REBCO tape for DC transport current I_{trans}=0.1I_c, 0.3 I_c, 0.5 I_c and 0.8 I_c under the 50 mT magnetic field with the frequency of 50hz. It can be observed that the dynamic resistance voltage goes higher and higher with the DC transport current increasing. For DC transport current I_{trans}=0.1 I_c, 0.3 I_c, 0.5 I_c, the dynamic resistance voltage could recover to zero. However, when the DC transport current reaches 0.8 I_c, the response could not recover to zero immediately. The delay in voltage recovery is due to the simulation calculation carried out using Jc(B) model, indicating the DC transport current has been above the level of real critical current of the superconductor currently.

After carrying out Fourier analysis of the waveform of the dynamic resistance voltage in Fig. 6, the DC component and second harmonics are obtained. As shown in Fig. 7, the blue curve with solid triangle, the green curve with hollow triangle and the red curve with circle represents the DC component, the second harmonic component and the ratio of above two components. It's apparent that the DC component and the second harmonics are increases with the value of DC transport current approaching to the critical current of the superconductor. The ratio of the DC component and the second harmonic component keeps increasing as well, which indicates that the increasing speed of DC component is larger than that of second harmonic component.

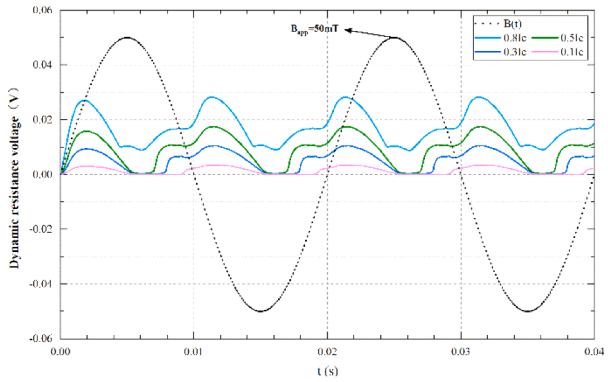

Fig. 6. The instantaneous dynamic resistance voltage of the REBCO tape under AC magnetic fields with amplitude B_{app}=50 mT for DC transport current I_{trans}=0.1I_c, 0.3 I_c, 0.5 I_c and 0.8 I_c.

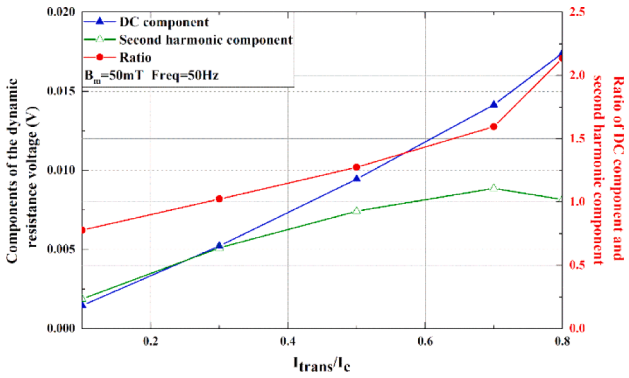

Fig. 7. The DC component, second harmonic component and ratio of the DC component and second harmonic component for the REBCO tape response voltage under 50 mT AC fields when DC transport current I_{trans}=0.1 I_c, 0.3 I_c, 0.5 I_c and 0.8 I_c.

4. Discussion

According to the analysis and simulation results above, the dynamic resistance voltage of the DC-carrying REBCO tape is positively related with its DC transport current and the amplitude and frequency of applied AC field. Although the DC component and the second harmonic component of the dynamic resistance voltage follow the dynamic resistance voltage to increase, the two components don't behave proportionally. The differences in the behavior of the two components could be displayed by the ratio of the two components. Specifically, if the DC transport current or amplitude of the AC magnetic field increases, the ratio of DC component and second harmonic component grows quickly, indicating the DC increases faster than the second harmonic component. By contrast, when the frequency of the AC magnetic field varies, the ratio of the DC component and the second harmonic component will maintain stable, which suggest the two components change in proportion.

In real HTS devices, the REBCO tapes usually operate in different AC magnetic field. The real critical current of the REBCO tapes are different under various AC field. Under the complex situation, if the DC transport current approaches the real critical current of the superconductor, the ratio of the DC component and second harmonic component will sensitively increase in response. Hence, the state of the superconductor could be monitored through obtaining the ratio of the two components, and the undesired quench could be sensed in advance.

5. Conclusion

In this paper, the waveform of the instantaneous dynamic resistance voltage has been simulated and depicted using the FEM model based on ***H***-formulation. Through Fourier analysis of the waveform of the instantaneous dynamic resistance voltage, value of two main components contained in the dynamic resistance voltage, the DC component and the second harmonic component, could be obtained. Under the circumstance when applied AC field or the DC transport current changes, these two components will response differently. The ratio of the two components could be utilized to reflect the change in external conditions and to monitor the state of the superconductor.

Declaration of Competing Interest

The authors declare that they have no known competing financial interests or personal relationships that could have appeared to influence the work reported in this paper.

References

[1] S. Dai, T. Ma, Q. Qiu, Z. Zhu, Y. Teng, L. Hu, Development of a 1250-kVA superconducting transformer and its demonstration at the superconducting substation, IEEE Trans. Appl. Supercond. 26 (1) (Jan. 2016). Art. no. 5500107.
[2] Y.-G. Kim, S. Hahn, K.L. Kim, O.J. Kwon, H. Lee, Investigation of HTS racetrack coil without turn-to-turn insulation for superconducting rotating machines, IEEE Trans. Appl. Supercond. 22 (3) (Jun. 2012), 5200604.
[3] B. Li, C. Li, F. Guo, Y. Xin, C. Wang, X. Pang, Coordination of superconductive fault current limiters with zero-sequence current protection of transmission lines, IEEE Trans. Appl. Supercond 24 (5) (2014) 1–5.
[4] P. Tixador, C. Villard, Y. Cointe, DC superconducting fault current limiter, Supercond. Sci. Technol. 19 (2006).
[5] S. Hahn, et al., 45.5-tesla direct-current magnetic field generated with a high-temperature superconducting magnet, Nature 570 (Jun. 2019) 496–499.
[6] V.V. Andrianov, V.B. Zenkevich, V.V. Kurguzov, V.V. Sychev, F. F.Ternovskii, Effective resistance of an imperfect type-II superconductorin an oscillating magnetic field, Soviet Phys. JETP 31 (1970) 815.
[7] M. Risse, M. Aikele, S. Doettinger, R. Huebener, C. Tsuei, M. Naito, Dissipation in the superconducting mixed state in the presence of a small oscillatory magnetic-field component, Physical Review B 55 (22) (1997) 15191.
[8] G.P. Mikitik, E.H. Brandt, Generation of a dc voltage by an ac magnetic field in type-II superconductors, Physical Review B 64 (9) (2001), 092502.
[9] E.H. Brandt, G.P. Mikitik, Why an ac magnetic field shifts the irreversibility line in type-II superconductors, Physical review letters 89 (2) (2002), 027002.
[10] T. Ogasawara, K. Yasukochi, S. Nose, H. Sekizawa, Effective re-sistance of current-carrying superconducting wire in oscillating magnetic fields 1: Single core composite conductor, Cryogenics 16 (Jan. 1976) 33–38.

[11] M.P. Oomen, Dynamic resistance in a slab-like superconductor with Jc(B) dependence, Supercond. Sci. Technol. 12 (Feb. 1999) 382–387.
[12] B. Shen, C. Li, G. Jianzhao, D. Qihuan, M. Jun, J. Gawith, T.A. Coombs, Investigation on Power Dissipation in the Saturated Iron-core Superconducting Fault Current Limiter, IEEE Transactions on Applied Superconductivity 29 (2) (2019), 5600305.
[13] C. Li, et al., Design for a persistent current switch controlled by alternating current magnetic field, IEEE Trans. Appl. Supercond. 28 (4) (Jun. 2018). Art. no. 4603205.
[14] J. Geng, C. Li, T.A. Coombs, A fast AC field controlled impedance in HTS coated conductors: Response speed and electric field value, IEEE Trans. Appl. Supercond. 27 (6) (Sep. 2017). Art. no. 5000305.
[15] C. Li, J. Geng, B. Shen, J. Ma, J. Gawith, T.A. Coombs, Investigation on the transformer-rectifier flux pump for high field magnets, IEEE Trans. Appl. Supercond. 29 (5) (Aug. 2019). Art. no. 4301105.
[16] J. Geng, T.A. Coombs, Mechanism of a high-Tcsuperconductingflux pump: Using alternating magnetic field to trigger flux flow, Appl.Phys. Lett. 107 (Oct. 2015), 142601.
[17] Z. Jiang, R. Toyomoto, N. Amemiya, X. Zhang, C.W. Bumby, Dy-namic resistance of a high-Tc coated conductor wire in a perpendicular magnetic field at 77K, Supercond. Sci. Technol. 30 (Jan. 2017). Art.no. 03LT01.
[18] Z. Jiang, et al., Dynamic resistance measurements in a GdBCO-Coatedconductor, IEEE Trans. Appl. Supercond. 27 (4) (Jun. 2017). Art. no. 5900205.
[19] Z. Jiang, Impact of flux gap upon dynamic resistance of a rotating HTS flux pump, Supercond. Sci. Technol. 28 (Sep. 2015). Art. no. 115008.
[20] Q. Li, M. Yao, Z. Jiang, C.W. Bumby, N. Amemiya, Numerical modeling of dynamic loss in HTS-coated conductors under perpendicular magnetic fields, IEEE Trans. Appl. Supercond. 28 (2) (Mar. 2018). Art. no. 6600106.
[21] M.D. Ainslie, et al., Numerical modelling of dynamic resistance in high-temperature superconducting coated-conductor wires, Supercond. Sci. Technol. 31 (7) (2018). Art. no. 074003.
[22] J. Ma, J. Geng, W.K. Chan, J. Schwartz, T.A. Coombs, A temperature-dependent multilayer model for direct current carrying HTS coated-conductors under perpendicular AC magnetic fields, Supercond. Sci. Technol. 33 (4) (2020). Art. no. 045007.
[23] Z. Hong, A.M. Campbell, T.A. Coombs, Numerical solution of critical state in superconductivity by finite element software, Supercond. Sci. Technol 19 (12) (2006). Art. no. 1246.
[24] B. Shen, C. Li, J. Geng, X. Zhang, J. Gawith, J. Ma, Y. Liu, F. Grilli, T.A. Coombs, Power dissipation in HTS coated conductor coils under the simultaneous action of AC and DC currents and fields, Supercond. Sci. Technol. 31 (7) (2018).
[25] B. Shen, F. Grilli, T.A. Coombs, Review of the AC Loss Computation for HTS using H formulation, Supercond. Sci. Technol. 33 (3) (2020).
[26] B. Shen, F. Grilli, T.A. Coombs, Overview of H-formulation: A versatile tool for modelling electromagnetics in high temperature superconductor applications, IEEE Access 8 (2020).